Chapter 3

Development of an in Vitro Anticancer Vaccine Platform Using Gold Nanoparticles Immunoconjugates

Teodora Mocan[1], Flaviu A. Tabaran[2], Cristian Matea[3], Teodora Pop[3], Diana Gonciar[3], Ofelia Mosteanu[3], Lucian Mocan[3], Dana Bartos[3], Lucia Agoston-Coldea[4], Cornel Iancu[3]

[1]Department of Physiology, "Iuliu Hatieganu" University of Medicine and Pharmacy, Clinicilor 5-7, Cluj-Napoca, Romania

[2]Department of Pathology, University of Agricultural Sciences and Veterinary Medicine, Faculty of Veterinary Medicine, 3-5 Manastur Street, 400372 Cluj-Napoca, Romania, tel/fax: +40264-593792

[3]Gastroenterology Institute; "Iuliu Hatieganu" University of Medicine and Pharmacy, 19-21 Croitorilor Street, Cluj-Napoca, Romania

[4]Department of Medical Sciences, Iuliu Hatieganu University of Medicine & Pharmacy, 2–4 Clinicilor, 400006, Cluj-Napoca, Romania

Introduction

Colon cancer is a major cause of deaths worldwide, and it is expected to rise in the coming years. Current therapeutic strategies in colon cancer treatment include surgical resection of the primary tumor, chemotherapeutic drugs and radiotherapy. (1, 2)

The development of nanoscale drug delivery systems represents an exciting and new approach to cancer treatment. (3) A strong goal in the use of nanoscale drug delivery systems is to deliver high doses of active bio-nanomolecules at specific sites while simultaneously reducing systemic toxicity. Very recent clinical trials suggest that nanoscale drug delivery systems such as Doxil® (doxorubicin encapsulated in liposomes (4) and Abraxane® (paclitaxel attached to nanoparticles) (5) could prolong survival in advanced cancer. One remarkable property of these nano-systems is represented by the activation of the immune system, which could form an attractive basis for cancer vaccine

development. Although such drug delivery systems hold a tremendous potential for the future prevention of cancer, the research for a true anticancer vaccine remains elusive. Nanotechnology has already brought to light promising results in the field of anticancer vaccines. For instance, inert nanobeads, recombinant virus-like particles (VLPs), and immunostimulating complexes, are being used in cancer vaccine research due to their efficacy at eliciting both cellular and humoral immune responses.

During the last decade, advances in functionalization chemistry have been one of the driving forces in the development of new classes of nanoparticles for applications in biology and medicine. (9). Due their unique physical and chemical properties nanosize particles hold great hopes for drug delivery and cancer therapy. (10). There are several encouraging data that some classes of nanostructures may be used in initiating and maintaining immune responses. (11). When bound to tumor antigens, they elicit a specific antitumor response in animal models. (12) Furthermore, data shown that peptide-functionalized nanoobjects can act as proficient immunomodulators and consequently generate specific antibody responses. (13) Moreover, ex vivo clonal expansion of T cells with antibody-linked nanoparticles results in T-cell activation and might lead to the development of novel immunotherapies. (14).

It has been shown in animal models that significant lymphocytes proliferation and secretion of cytokines may help to rebuild the host`s immunity against cancer and consequently to generate obvious antitumor immunity. Despite their proven role in proliferation of T lymphocytes, especially the proliferation of $CD8^+$ lymphocytes (cytotoxic T lymphocytes) (14) which constitutes the main part of antitumor effector cells (15), (16) there are currently no studies that explore the concept of cancer prophylaxis mediated by gold nanoparticles.

Recent literature data supports the role of embryonic stem cells (ESC) as

cellular cancer vaccine that stimulates the biological systems to destroy colon cancer cells by eliciting an immune boost. (17). The implication is supported by the fact that ESC prevent and control the proliferation and expansion of malign tumors in vivo by formation and development of CD^+ and $CD8^+$ T lymphocytes (18). Considering all these data together we have been recently able to demonstrate that combined administration of both ESC and multi walled carbon nanotubes can function as powerful nanobiosystem to induce and rebuild antitumor immunity in colon tumor animal models. (Figure 1). The proposed administration led to significant antitumor responses and enhanced tumor rejection in mice with subcutaneous inoculation of colon malign cells. (19) The paper was published in Journal of American Society for Nanomadicine and was the first paper that introduced a novel concept in the field: that of nano-mediated anti-cancer vaccine.

Still, toxicity issues regarding carbon nanotube-living organism interaction, have been suggested by our data (20-25) and other research groups reports. (26, 27) Reports suggest carbon nanotubes might be unnappropriate for long-term human usage. Recently, gold nanoparticles were approved on human treatment in phase 1 clinical trials, which suggests that gold can act as an effective and safe agent for human-intend applications. (www.clinicaltrials.gov). Present project proposes tailoring of research from a clinical perspective by using gold nanoparticles (that are approved for human treatment) in order to develop a novel prophylaxy method for colon cancer.

Moreover, preliminary obtained results suggest that nanostructures may function as antigen presenting molecules. We have, therefore, reasoned that binding of a low immunogenic peptide antigen onto the gold nanoparticle could lead, by presentation to MHC molecules of dendritic cells, to an essential mount in immune response intensity. We reason that MUC1 (CD227), a

membrane-tethered mucin glycoprotein that is normally expressed on the apical surfaces of normal glandular epithelia, could become an adequate conjugator for Gold-NPs., capable to produce the expected effect. It has been previousely stated that MUC 1 is over expressed and aberrantly glycosylated in >70% of human colon cancer. (28) Recent description of MUC1 as a target for cytotoxic T lymphocytes (CTLs) has raised interest in using this protein as a possible target for immunotherapy, suggesting a good potential for its application of nanomediated colon cancer vaccine. (29-31)

Additionaly, based on previous experiments, we reason that changing the initial vaccine formulation through in vitro pre-pulsing of embryonic stem cells to facilitate dendrite cell differentiation would make a difference in the final desired in vivo effect following administration.

We therefore hypothesize that a novel vaccine nano-formulation, containing MUC-1- functionalized GoldNPs and stem cell-derived dendritic cells could lead to potent antitumor lymphocyte activation, thus opening new avenues in the prophylaxy of colon cancer.

Motivation

MUC1 (CD227) is a membrane-bound glycoprotein expressed in normal glandular epithelial cells under basal conditions. Existing studies in the literature suggest MUC1 overexpression and aberrant glycosylation in more than 70% of colorectal cancers. Recent studies focus on its potential to serve as target for cytotoxic T lymphocytes. The use of MUC1 in immunotherapy as a specific target gives way to potential applications in nanoparticle-mediated therapies for colorectal cancer.

Exposure of dendritic cells to MUC1-gold nanoparticle conjugates aims to

stimulate MUC-1 antigen presentation to specific immune cells (lymphocytes), regulated by the major histocompatibility complex (MHC). The intended response is to induce peptide-specific immune activation with improved anticancer effect. The final formula of the vaccine against colorectal cancer combines the effect of three factors which have already proven their efficacy in immunostimulation: gold nanoparticles, dendritic cells and the tumor-specific peptide (MUC1).

A MUC1-specific proteic product (ab 80082) was selected for the experiment. Product selection was based on similar experiments in the literature, employing structure-based binding methods. The presence of a histidine residue (His) in the selected molecule makes the functionalization of gold nanoparticles with bio-ligands theoretically approachable and guarantees future binding success.

Microscopic Assessment of Dendritic Cell Cultures

Analysis of Dendritic Cell Cultures by Optical Microscopy

Cell culture plates and adherent dendritic cell cultures on port object slides were examined using an optical microscope (Olympus BX51). Simple optical and phase contrast microscopy images were obtained using an Olympus SP-350 camera and processed with Cell B Olympus and Olympus Stream Basic programs.

Analysis of Dendritic Cell Cultures by Laser Scanning Confocal Microscopy

Dendritic cell cultures obtained were analyzed and characterized using Zeiss LSM 710 confocal microscope mounted on an inverted microscope (Axio Observer Z1). EC plan neofluar 10x/0.30M27 objectives were used to

obtain an overview of cell cultures and plan apochromat 63x/1.40 objectives were used to observe structural details of dendritic cells. The lasers used to obtain specific fluorochrome excitation emitted light at 488 nm and 633 nm. Both argon laser and helium-neon laser were set to 5.0% of their light potential. Laser beam aperture (aperture/"pinhole") was fixed at 39 μm (1 Airy unit) for images obtained with x10 objectives and 50 μm for 63x objectives.

For images obtained with the 63x objective, the main acquisition for fluorescence channel 1 (green channel-FITC) was 945, and 570 for channel 2 (red DRAQ5).

For images obtained with 10x objective, the main acquisition for fluorescence channel 1 (green channel-FITC) was 834, and 871 for channel 2 (red DRAQ5). Digital amplification of the fluorescent signal was 15 for Ch1 and 1 for Ch2.

Laser beams were generated at 492-629 nm for fluorescence channel 1 and 661-757 for fluorescence channel 2.

Histochemical and Immunohistochemical Staining of Dendritic Cell Cultures for Laser Scanning Confocal Microscopy

Immunocytochemistry (indirect immunofluorescence) was employed to examine CD68 cell membrane antigen expression, using an anti-CD68 polyclonal antibody (IgG) (product Linaris Biologische Produkte, catalog no. MAK0341Q). Visualization was performed via fluorescent staining with fluorescent secondary antibody conjugates. Annex 1 shows the immunocytochemical staining protocol used. Histochemical labeling with fluorochrome DRAQ5® was used in order to visualize nuclei from the cell culture (Cell Signaling Technology Product, Cat. No. 4084).

The cytoskeleton was viewed using selective labeling of actin fibers. Labeling was performed by incubating fixed cells permeabilized with phalloidin (isolated from Amanita phalloides) and conjugated with FITC fluorochrome (Sigma-Aldrich product, Cat. No. 5282). Annex 2 shows the phalloidin labeling protocol used.

Results

Analysis of Dendritic Cell Cultures by Optical Microscopy

Cell cultures analyzed using simple optical microscopy and phase contrast or dark field microscopy reveal the presence of stellate cells (dendritic) with 3-5 branches (most cells observed) or fusiform cells (rare), adherent to culture flask walls (Figure 1). Cell growth occurs in a single and relatively uniform layer, with different degrees of confluence depending on the duration of the growth process. Cellular extensions have different lengths, from a few microns, which give a scalloped aspect to the edge of the cell, to over 20 μm. Rare cells are spherical or oval. Most cells are large, with an average length of 40-70 μm, including dendritic extensions. Cell body varies in volume, with a bulky round or oval central nucleus. Bilobed-reniform nuclei were rare. Some cells contain two adjacent nuclei (binucleated cells). The cytoplasm of cells with dendritic morphology is finely granular or, in some cases, finely vacuolated. There was a small percentage of suspension cells, generally oval-shaped.

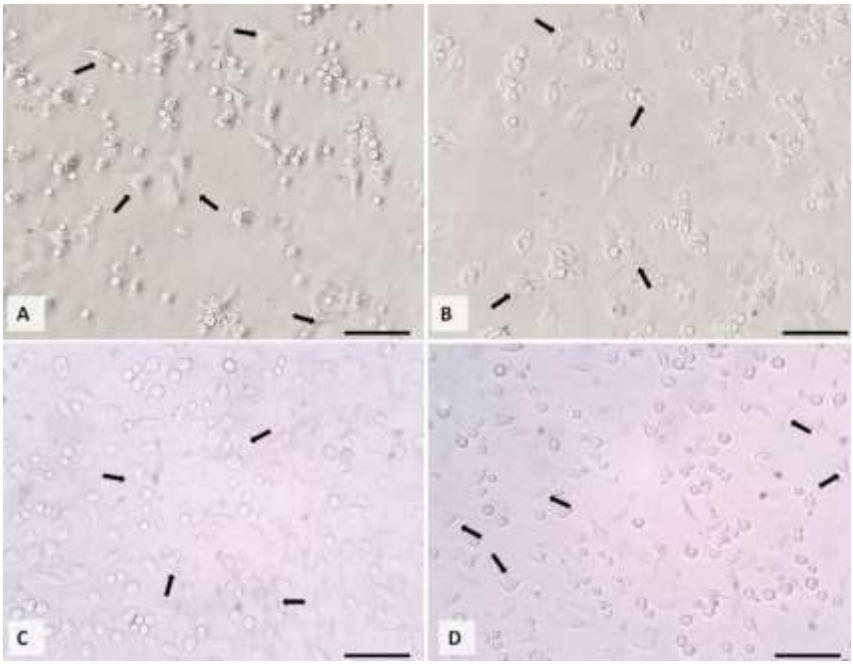

Figure 1. *Images of phase contrast microscopy (images A and B) and simple optical microscopy (images C and D) of isolated dendritic cell cultures. The arrows indicate cells with morphology that is characteristic of dendritic cells. Scale: 100 μm.*

Analysis of Dendritic Cell Cultures by Laser Scanning Confocal Microscopy

Cell culture analysis using laser scanning confocal microscopy confirms the dendritic morphology observed by optical microscopy, but adds essential data regarding cell structure. Dendritic extensions contain large numbers of actin filaments, following the path of these extensions along their entire length (Figure 2). These extensions sometimes end with a fine edge of side branches also containing actin in the cytoskeleton. The nucleus is oval, with compact or coarse chromatin and variable nucleolus (invisible for about half of the cells analyzed). Actin clusters can sometimes appear on the dendritic cell body (small size, 1-2 μm), giving cells a granular appearance.

Monolayer cell growth is generally observed on the entire surface of the culture plates, with the exception of certain outbreaks where dendritic cells are overlapped, with a bud-pattern aspect (colonies), consisting of 5 to 20 cells. Cellular debris with globular appearance, containing traces of DNA and actin (apoptotic bodies), are rarely observed.

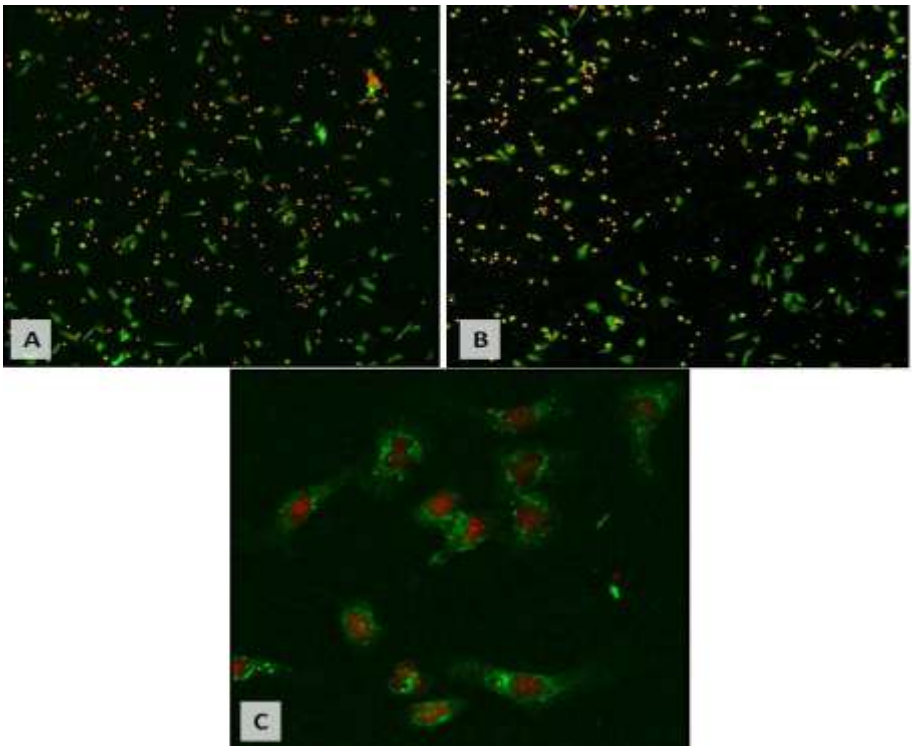

Figure 2. *Laser confocal microscopy images of dendritic cell cultures. The specific fluorescence of fluorochrome-labeled (DRAQ5) cell nuclei is observed in the red fluorescent channel. The fluorescence of phalloidin-conjugatedFITC-labeled actin fibers is observed in the green channel. Images A and B were obtained with a Plan Neofluar 10x/0.30 M27 Objective, and image C with a Plan Apochromat 63x/1.40 Objective.*

Expression of dendritic cells for CD68 antigen was stable and obvious for most cells analyzed. In terms of distribution, the antigen had a typical location, in the membrane, sometimes granular and insular. There was a small or medium

amount of antigen expression for most cells with dendritic morphology. CD68 antigen expression also occurred for spherical or oval cells (Figure 3).

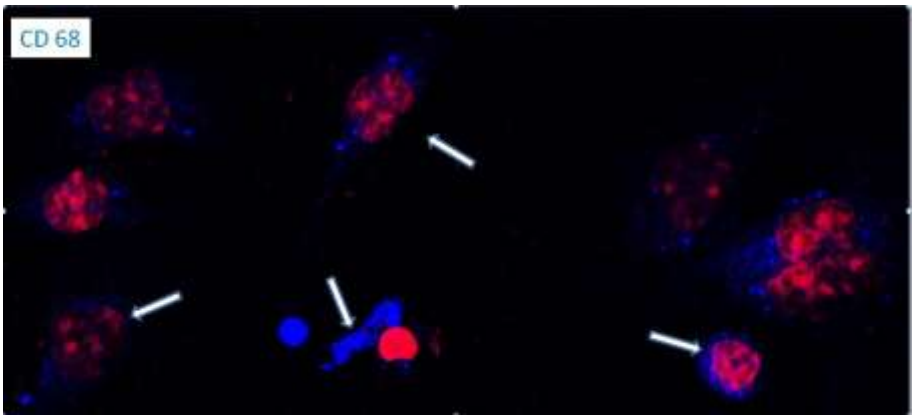

Figure 3. *Laser scanning confocal microscopy images of dendritic cell cultures immunocytochemically labeled with CD68 antigen. Blue fluorescence channel shows the positive CD68 antigen expression by cells with dendritic morphology. Red fluorescence channel shows the specific fluorescence of fluorochrome-labeled (DRAQ5) cell nuclei. Plan Apochromat 63x/1.40 Objective.*

Annex 1. *Immunocytochemical staining for CD68 antigen.*

1	Fixation with anhydrous acetone at -20 ℃	5 minutes
2	Phosphate buffered saline (PBS) washing	3 x 1 minute
3	Blocking non-specific binding by incubation with 3% BSA in phosphate buffered saline (PBS)	10 minutes
4	Incubation with primary antibodies (anti-CD 68)	3 hours at 37 ℃
5	Phosphate buffered saline (PBS) washing	3 x 1 minute
6	Incubation with secondary antibodies	30 minutes at 37 ℃
7	Phosphate buffered saline (PBS) washing	3 x 1 minute
8	Incubation with DRAQ5®	5 minutes
9	Phosphate buffered saline (PBS) washing	3 x 1 minute
10	Adding Mowiol mounting medium	

Discussion

Dendritic cells are antigen-presenting cells playing a key role in regulating

the adaptive immune responses, achieving peripheral antigen uptake and processing. Further, by blood or lymphoid migration into lymphatic tissues rich in T lymphocytes, they present antigens to lymphocyte populations undergoing the execution stage of immune responses. Besides controlling the induction of the primary immune response, DCs are also essential for the induction of immunological tolerance.

Mature dendritic cells are isolated and characterized based on their key morphological properties in vivo and in vitro, as well as on the expression of different functional antigens. Considering that there is not only one antigen identifying dendritic cells, their phenotyping implies the characterization of a broad package of molecules. Dendritic cells and their subtypes are characterized by the presence or lack of major histocompatibility complex class II molecules, CD68 antigens, CD83, p55, S100b, M342i, MIDC-8, CD11c, CD123 and the absence of certain antigens such as CD3, CD14, CD19, CD56 and CD66b.

Regarding the expression of CD68 antigen expression found here, it is an important tool in diagnosing monocytes/macrophages and dendritic cells. Even if it is usually used to identify monocytes/macrophages, this antigen is also expressed by other cells, such as endothelial cells or fibroblasts, but in a variable quantity, much smaller than macrophages or dendritic cells. Thus, a powerful expression of this antigen is a characteristic of macrophage cells and dendritic cells derived from the myeloid cell line. Moreover, not only the expression, but the location of CD68 is suggestive for immunophenotyping. While macrophages are mainly located intracytoplasmically or around the cell membrane, dendritic cells have a predominant perinucelar CD68 location.

From a morphological point of view, one of the most important features employed for the identification and characterization of dendritic cells, is represented by the multiple cytoplasmic extensions that give a stellate

appearance to these cells. The number and characteristics of these extensions vary depending on the degree of maturity (differentiation) and the medium where cells are described (in vivo/in vitro). Mature dendritic cells in culture flasks visualized by phase contrast microscopy have various cell extensions (over 10 μm long) giving cell edges a veil look. The morphological aspect observed by means of optical and confocal microscopy is suggestive of dendritic cell characteristics. The long multiple or branched extensions are typical dendritic cell characteristics, and even more, they are characteristics of semi-mature or mature dendritic cells.

Actin fibers reinforce the cell skeleton, becoming one of the most important consolidation elements for dendritic cell extensions spines bet on our case. Because of this, actin skeleton analysis brings important information on cellular ramifications. Furthermore, due to its major role in cell mobility and dendritic cell development, the amount of actin is suggestive of the movement capacity and of the ability to infer the prevailing phagocitary activity or antigen presentation.

Even if both immunocytochemical and microscopic observations are characteristic of dendritic cells, complementary immunophenotyping studies are required for complete phenotyping and determination of the degree of maturity/differentiation.

Conclusion

Optical and laser scanning confocal microscopy observations of culture plates suggest dendritic cell morphology under various stages of differentiation/maturity.

Analyzed cells exhibit intense immunopositivity for CD68 antigen, a typical property of monoblast-derived cells, namely dendritic cells and monocytes/macrophages.

Functionalization of Gold Nanoparticles with MUC1

Synthesis of gold nanoparticles was performed in aqueous medium using the Turkevich method, with a few minor changes. Briefly, 48 mg of $HAuCl_4$ (Sigma-Aldrich code 520918) were dissolved in 100 mL bidist H_2O. Further, 100 mg sodium citrate (Sigma-Aldrich code S4641) were dissolved in 5 mL bidist H_2O, the resulting solution being subjected to ultrasounds for 15 minutes. The citrate solution obtained was heated to 100 ℃ and then the $HAuCl_4$ solution was quickly added, under continuous magnetic stirring. Under the action of temperature and citrate,

Au (III) was reduced to Au^0 (metallic gold). The reaction was allowed to proceed to reflux for 2 hours. Then, the solution was cooled to room temperature, subjected to centrifugation (15,000 rpm for 30 minutes) and redispersed in bidist H_2O using a sonicator. Assessment of citrate-stabilized gold nanoparticles (GNPs) was performed using a Shimadzu 1800 UV-Vis spectrophotometer. Synthesized gold nanoparticles showed a reddish coloration and a maximum absorption of λmax = 523nm.

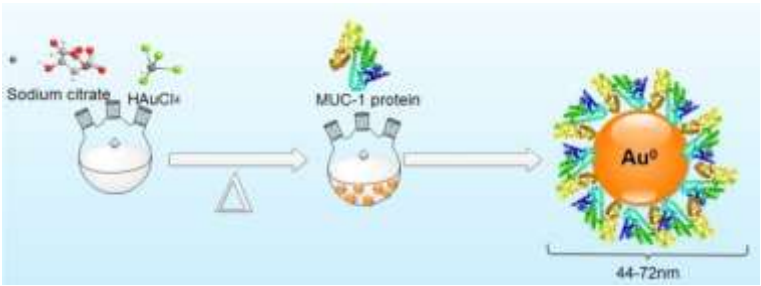

Figure 4. *Functionalization of gold nanoparticles with MUC1.*

For functionalization of gold nanoparticles with MUC1, the latter was reduced in the presence of dithiothreitol (DTT). Briefly, 150 µL MUC1 solution (conc. 1 µg/µL) were dispersed in 1 mL bidist H_2O, to which 400 µL 100 mM

DTT solution (pH=8.5) were added and the sample was incubated for 1 hour at room temperature. The reduction step is designed to break the disulfide bonds inside the protein and to expose thiol groups (-SH), groups with affinity for the synthesized gold nanoparticles. Further, the reduced MUC1 solution was combined with 5 mL GNP solution, pH was adjusted to ≈7 and the reaction was allowed to proceed for 2 hours at room temperature. It is now that the sample color changed from red to blue (Figure 5). This change in color is due to MUC1 attachment to gold nanoparticles.

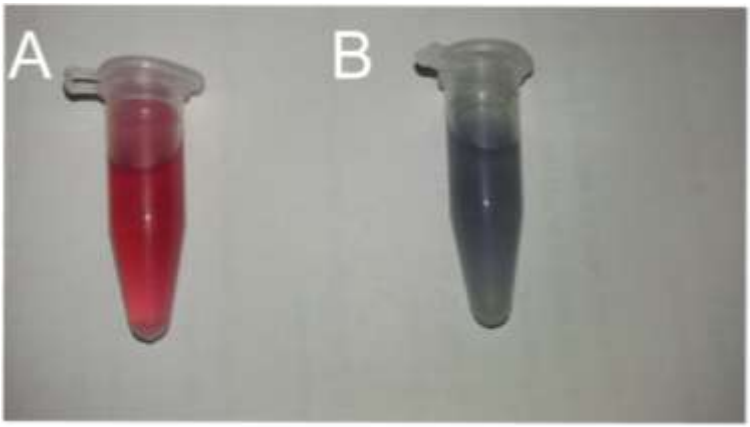

Figure 5. *A - GNP solution; B - GNP solution in reaction to reduced MUC1.*

Gold nanoparticles functionalized with MUC1 (MUC1-GNPs) were subjected to centrifugation (15,000 rpm for 15 minutes) and re-dispersed by sonication in bidist H_2O to remove secondary reaction products.

Characterization of the Newly Obtained MUC1-GNP Compounds

The MUC1-GNP solution was characterized using spectral methods (UV-Vis) and atomic force microscopy (AFM).

UV-Vis spectra of GNPs and MUC1-GNPs were recorded using a Shimadzu 1800 spectrophotometer and normalized using OriginLab ™ software.

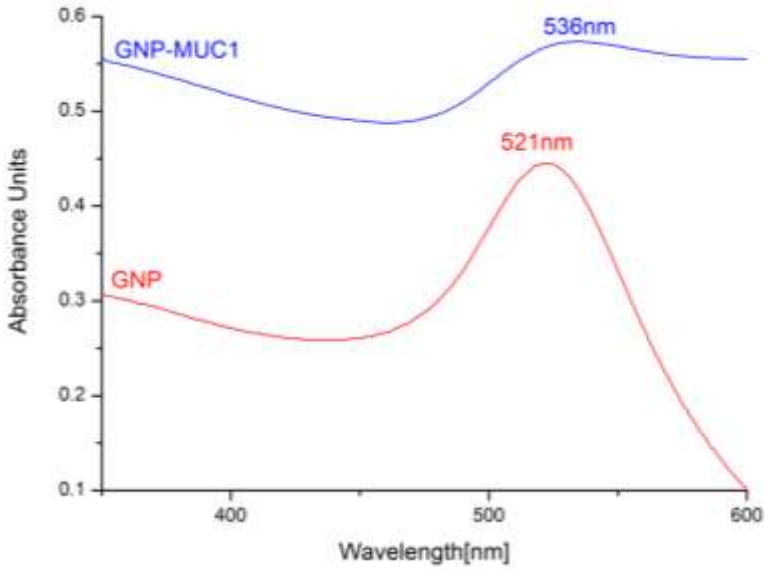

Figure 6. *UV-Vis spectra of GNPs and MUC1-GNPs.*

Figure 6 shows that the spectrum of GNPs exhibits a GNP-specific absorption maximum of λmax=523 nm. The absorption maximum for MUC1-GNPs suffers a bathochromic effect, with a λmax = 536 nm.

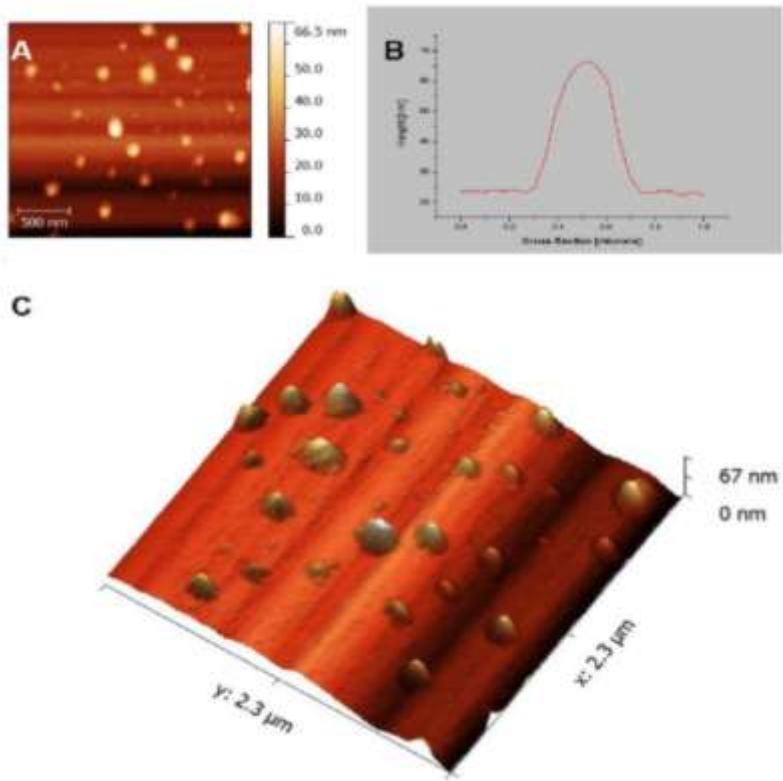

Figure 7. *AFM images of MUC1-GNPs. A - 2D topographic image; B - MUC1-GNP profile; C -3D representation.*

Nanoparticles functionalized with MUC1 were analyzed using atomic force microscopy (TT- AFM Workshop™ microscope). Samples were previously dispersed with a in-sample sonicator and deposited on a Mica structure. Data acquisition was performed under non-contact mode (vibrating mode). Data were processed using Gwyddion® software. Nanoparticle size was calculated based on profiles extracted from images, MUC1-GNP ranging between 44 and 72 nm (Figure 7B). Figure 7C shows a three-dimensional representation of functionalized nanoparticles.

Exposure of Dendritic Cells to MUC1-GNPs in Vitro

Cell Culture Preparation

For the microscopic examination of cells, seeding was performed (after trypsinization, detachment and passage) on slides with 4 separate chambers (four well-chamber), corresponding to the four groups. After cell reattachment and growth in specific medium (0.5 ml/chamber), cells were serially counted, identifying the exponential growth phase.

Cell cultures carried out to test cell proliferation were obtained by cell seeding in 96-well plates (50 microliters/well).

Cell Exposure to the Material

At the appropriate time, cells were exposed by adding 0.5 ml of test solution in each chamber on the microscope slide, and 50 microliters in each well of the 96-well plate, as follows:

1 Group 1 - unexposed (culture medium)

2 Group 2 - exposed to MUC1-GNPs in low concentration (5 micrograms/mL)

3 Group 3 - exposed to MUC1-GNPs in average concentration (10 micrograms/mL)

4 Group 4 - exposed to MUC1-GNPs in high concentration (20 micrograms/mL)

Incubation with the corresponding test solution was performed for 2 hours under standard conditions (37 ℃, 5% CO_2).

For the quantification of cell proliferation, experiments were carried out in triplicate, each group being assigned three wells out of the existing 96 wells on the plate.

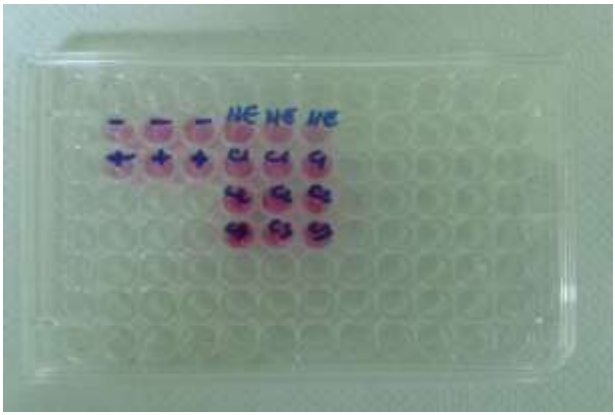

Figure 8. *Aspect of 96-well-plate including MUC-1-GNPs- exposed and non-exposed groups, as well as positive and negative controls.*

Quantification of Cell Proliferation/Viability

The assessment of the effects of cell exposure to various solutions on cell viability was performed using MTT Assay protocols. The

MTT reagent (3-(4,5-dimethyl-2-thiazolyl)-2,5-diphenyl-2H-tetrazolium bromide) is a compound that undergoes reduction processes in metabolically active cells (viable cells). The resulting compound, formazan, can be solubilized and quantified using spectrophotometry. The specific protocol of the manufacturer (ATCC) was used in order to assess cell viability and proliferation. Briefly, it follows the succeeding growth steps using specific culture media mentioned above, with MTT reagent addition, incubation for 2-4 hours until the formation of visible precipitates, addition of detergent substances, maintaining the solution in the dark for 2 hours at room temperature. Finally, counting was done spectrophotometrically at 570 nm. The results were expressed as a percentage of the levels reported for the control samples.

Results

After exposure, the cell culture aspect was examined microscopically.

The quantification of the level of cell proliferation/viability was also performed, considering 100% absorbance of the non-exposed batch (OD 570 nm).

As shown in the figure below, the levels of proliferation were constant, without significant differences between any of the 2 groups ($p>0.05$).

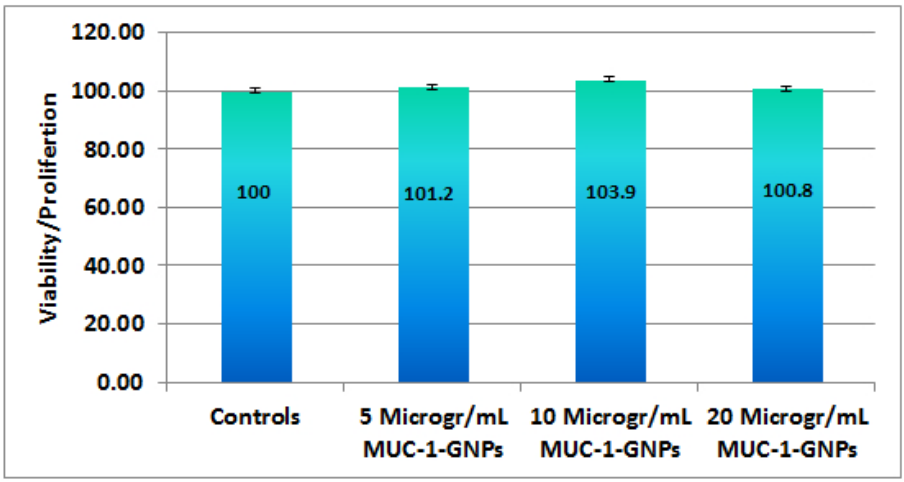

Figure 9. *MTT assay results for the exposed groups.*

Discussion

The experiments in the literature show mixed results regarding the cytotoxicity of the compounds obtained by covalent conjugation of gold nanoparticles with protein molecules. Thus, some studies indicate a definite toxicity, evidenced by the level of the half maximal inhibitory concentration measured by MTT and LDH assays. PCR experiments, as well as ATP

depletion dosage, suggest the induction of both intrinsic and extrinsic apoptotic cell damage. Strictly dependent on the attached molecules and other features of the nanomaterial, gold nanoparticles can interact with cellular DNA, redox balance, mutagenesis, and protein synthesis.

Other evidence suggests the absence of toxic effects on gold nanoaparticles of different sizes and functionalization agents: biotin, cysteine, glucose, etc., as demonstrated by the MTT assay (6).

The effects of gold nanoparticles on dendritic cells have recently been studied. The study demonstrates the lack of cytotoxic effects on this cell type of major importance in both humoral and cell-mediated immunity. The absence of any phenotypic change in dendritic cells suggests the absence of dendritic cell activation. However, an interesting observation of the study is provided by the intense changes in cytokine profile, which might induce future activation. (7).

Current experiments demonstrate the high level of biocompatibility of the newly synthesized product. The interaction between MUC1-GNPs and dendritic cells does not induce significant levels of apoptosis. This is particularly useful when intended to build a combined vaccine (cells + nanomaterial). It is also notable that in the absence of cytotoxic effects, the presence of MUC1 and the altered cytokine profile, already demonstrated in the literature, may contribute to cell activation required for immunostimulation.

Conclusion

Quantification of cell viability after exposure of PANC 1 cells indicates the lack of cytotoxic effects of the newly generated MUC1-GNPs nanoconstruct.

Assessment of MUC1-GNP Basal Cytotoxicity in Dendritic Cells

Both optical microscopy and confocal microscopy were used to assess the toxic changes and cell damage that may occur following exposure of dendritic cells to the test compound.

Optical microscopy observed that the analyzed cells retained their typical dendritic morphology after exposure to gold nanoparticles functionalized with MUC1. Furthermore, there were no changes in cell adhesion or cell morphology following exposure to 10 µg or 20 µg doses of MUC1-GNPs, cells also maintaining a similar morphology to control cultures (Figure 4).

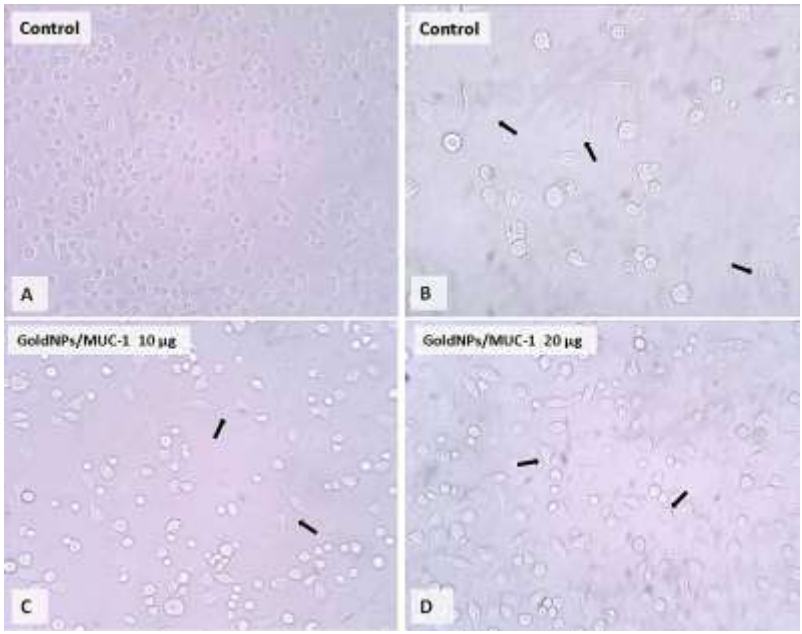

Figure 10. *Images of dendritic cell cultures isolated after exposure to different doses of gold nanoparticles functionalized with MUC1 (MUC1-GNPs), provided by optical microscopy. Arrows indicate cells with characteristic dendritic morphology in control cell cultures and following exposure to the test compound.*

Laser confocal analysis of dendritic cell cultures is in agreement with the information provided by optical microscopy. There were no changes suggesting a cytotoxic effect (i.e. cytoplasmic or nuclear vacuolation, cell ballooning, detachment from the adherent surface, cell wall fragmentation or decrease in the number or length of dendritic extensions). Therefore, dendritic cells retained their structure unchanged following exposure to 10 μg or 20 μg doses of MUC1-GNPs (Figure 11).

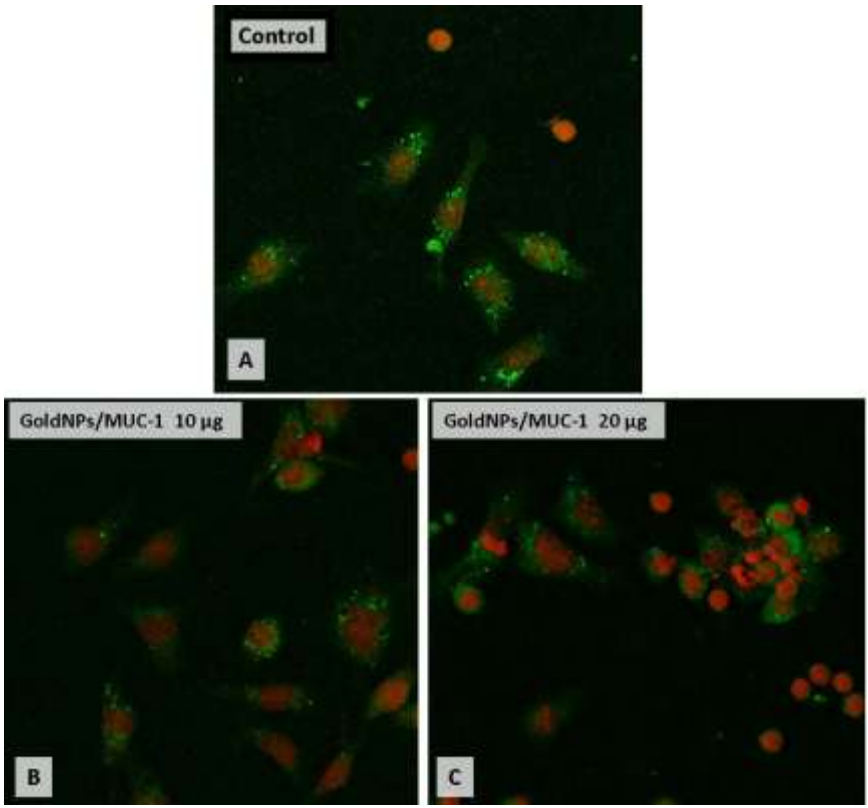

Figure 11. *Images of dendritic cell cultures isolated after exposure to different doses of gold nanoparticles functionalized with MUC1 (MUC1-GNPs), provided by laser confocal microscopy. Specific dendritic cell nuclei fluorescence (histochemically labeled with DRAQ5) is observed in the red fluorescence channel. Actin fiber fluorescence (labeled with FITC-conjugated phalloidin) is observed in the green channel. Images were acquired with a Plan Apochromat 63x/1.40 Objective.*

Conclusion

The microscopic analysis carried out after exposure suggests the high cellular biocompatibility of the newly synthesized product.

Annex 2. *Histochemical labeling of actin fibers in the dendritic cell cytoskeleton.*

1	4% paraformaldehyde fixation	10 minutes
2	Phosphate buffered saline (PBS) washing	3 x 1 minute
3	Tween 20 permeabilization (10% in PBS)	5 minutes
4	Phosphate buffered saline (PBS) washing	3 x 1 minute
5	Incubation with phalloidin (FITC) working solution	40 minutes in the dark
3	Phosphate buffered saline (PBS) washing	3 x 1 minute
8	Incubation with DRAQ5® for nuclei labeling	5 minutes
9	Phosphate buffered saline (PBS) washing	3 x 1 minute
10	Adding Mowiol mounting medium	

Conclusion

1. Experiments resulted in the generation and complex characterization of an innovative bionanocomposite product, MUC1-GNP.

2. When in contact with dendritic cells, key components of the future anti-cancer vaccine, the new product acts as a low-cytotoxic agent, recommended for cell/living tissue applications in a concentration of 0-20 micrograms/mL.

References

[1] Jemal A, Bray F, Center MM, Ferlay J, Ward E, Forman D. Global cancer statistics. CA Cancer J Clin 2011 Mar-Apr;61(2):69-90.

[2] Segal NH, Saltz LB. Evolving treatment of advanced colon cancer. Annu Rev Med 2009;60:207-219.

[3] Subramani K, Hosseinkhani H, Khraisat A, Hosseinkhani M, Pathak Y. Targeting nanoparticles as drug delivery systems for cancer treatment. Current Nanoscience 2009;5(2):135-140.

[4] ElBayoumi TA, Torchilin VP. Tumor-targeted nanomedicines: enhanced antitumor efficacy in vivo of doxorubicin-loaded, long-circulating liposomes modified with cancer-specific monoclonal antibody. Clinical Cancer Research 2009;15(6):1973.

[5] Miele E, Spinelli GP, Miele E, Tomao F, Tomao S. Albumin-bound formulation of paclitaxel (Abraxane® ABI-007) in the treatment of breast cancer. International Journal of Nanomedicine 2009;4:99.

[6] Bachmann MF, Jennings GT. Vaccine delivery: a matter of size, geometry, kinetics and molecular patterns. Nature Reviews Immunology 2010.

[7] Wang E, Monaco A, Monsurro V, Sabatino M, Pos Z, Uccellini L, et al. Antitumor vaccines, immunotherapy and the immunological constant of rejection. IDrugs 2009 May;12(5):297-301.

[8] Scheerlinck JPY, Greenwood DLV. Virus-sized vaccine delivery systems. Drug Discov Today 2008;13(19-20):882-887.

[9] Xu Y, Mahmood M, Fejleh A, Li Z, Watanabe F, Trigwell S, et al. Carbon-covered magnetic nanomaterials and their application for the thermolysis of cancer cells. Int J Nanomedicine 2010 Apr 7;5:167-176.

[10] Levi-Polyachenko NH, Merkel EJ, Jones BT, Carroll DL, Stewart JH, 4th. Rapid photothermal intracellular drug delivery using multiwalled carbon nanotubes. Mol Pharm 2009 Jul-Aug;6(4):1092-1099.

[11] Kostarelos K, Bianco A, Prato M. Promises, facts and challenges for carbon nanotubes in imaging and therapeutics. Nature Nanotechnology 2009;4(10): 627-633.

[12] Meng J, Duan J, Kong H, Li L, Wang C, Xie S, et al. Carbon nanotubes conjugated to tumor lysate protein enhance the efficacy of an antitumor immunotherapy. Small 2008;4(9):1364-1370.

[13] Pantarotto D, Partidos CD, Hoebeke J, Brown F, Kramer E, Briand JP, et al. Immunization with peptide-functionalized carbon nanotubes enhances

virus-specific neutralizing antibody responses. Chem Biol 2003;10(10):961-966.

[14] Fadel TR, Steenblock ER, Stern E, Li N, Wang X, Haller GL, et al. Enhanced cellular activation with single walled carbon nanotube bundles presenting antibody stimuli. Nano letters 2008;8(7):2070-2076.

[15] Begley J, Ribas A. Targeted therapies to improve tumor immunotherapy. Clinical Cancer Research 2008;14(14):4385.

[16] Rosenberg SA, Yang JC, Restifo NP. Cancer immunotherapy: moving beyond current vaccines. Nat Med 2004;10(9):909.

[17] Li Y, Yao Y, Sheng Z, Yang Y, Ma G. Dual-modal tracking of transplanted mesenchymal stem cells after myocardial infarction. Int J Nanomedicine 2011;6:815-823.

[18] Dong W, Du J, Shen H, Gao D, Li Z, Wang G, et al. Administration of embryonic stem cells generates effective antitumor immunity in mice with minor and heavy tumor load. Cancer Immunology, Immunotherapy 2010:1-9.

[19] Mocan T, Iancu C. Effective colon cancer prophylaxis in mice using embryonic stem cells and carbon nanotubes. International Journal of Nanomedicine 2011;6:1945.

[20] Mahmood M, Casciano DA, Mocan T, Iancu C, Xu Y, Mocan L, et al. Cytotoxicity and biological effects of functional nanomaterials delivered to various cell lines. Journal of Applied Toxicology 2010;30(1):74-83.

[21] Mocan T, Clichici S, Agoşton-Coldea L, Mocan L, Şimon Ş, Ilie IR, et al. Implications of oxidative stress mechanisms in toxicity of nanoparticles (review). Acta Physiol Hung2010;97(3):247-255.

[22] Mocan T, Clichici S, Biris AR, Simon S, Catoi C, Tabaran F, et al. Dynamic effects over plasma redox ballance following subcutaneous injection of single walled carbon nanotubes functionalized with single strand DNA. Dig J Nanomat Bios 2011;6(3):1207-1214.

[23] Iancu C, Mocan L, Bele C, Orza AI, Tabaran FA, Catoi C, et al. Enhanced laser thermal ablation for the in vitro treatment of liver cancer by specific delivery of multiwalled carbon nanotubes functionalized with human serum albumin. International Journal of Nanomedicine 2011;6:129.

[24] Mocan L, Tabaran F, Mocan T, Bele C, Orza A, Lucan C, et al. Selective ex-vivo photothermal ablation of human pancreatic cancer with albumin functionalized multiwalled carbon nanotubes. International Journal of Nanomedicine 2011 28 April 2011;6(1):915-928.

[25] Mocan T, Clichici S, Biris A, Simon S, Catoi C, Tabaran F, Et Al. Dynamic Effects Over Plasma Redox Ballance Following Subcutaneous Injection Of Single Walled Carbon Nanotubes Functionalized With Single Strand DNA.

[26] Zuzana M, Alessandra R, Lise F, Maria D. Safety Assessment of Nanoparticles Cytotoxicity and Genotoxicity of Metal Nanoparticles In Vitro. Journal of Biomedical Nanotechnology 2011;7(1):20-21.

[27] AshaRani P, Low Kah Mun G, Hande MP, Valiyaveettil S. Cytotoxicity and genotoxicity of silver nanoparticles in human cells. ACS nano 2008;3(2):279-290.

[28] Taylor-Papadimitriou J, Burchell J, Miles D, Dalziel M. MUC1 and cancer. Biochimica et Biophysica Acta (BBA)-Molecular Basis of Disease 1999; 1455(2-3):301-313.

[29] Brossart P, Schneider A, Dill P, Schammann T, Grünebach F, Wirths S, et al. The epithelial tumor antigen MUC1 is expressed in hematological malignancies and is recognized by MUC1- specific cytotoxic T-lymphocytes. Cancer Res 2001;61(18):6846.

[30] Noto H, Takahashi T, Makiguchi Y, Hayashi T, Hinoda Y, Imai K. Cytotoxic T lymphocytes derived from bone marrow mononuclear cells of multiple myeloma patients recognize an underglycosylated form of MUC1 mucin. Int Immunol 1997;9(5):791.

[31] Mukherjee P, Ginardi AR, Tinder TL, Sterner CJ, Gendler SJ. MUCl-specific cytotoxic T lymphocytes eradicate tumors when adoptively transferred in vivo. Cancer Res 2001;7(3 Supplement):848s.